

Vortex Generators

GROUP 7

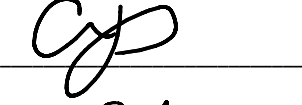
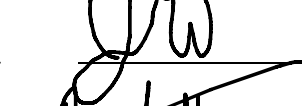
ASE – 120K Low-Speed Aerodynamics Laboratory

The University of Texas at Austin

Department of Aerospace Engineering and Engineering Mechanics

Spring, 2025

By signing this form, I acknowledge that I have read this entire document prior to submission, that I approve of all material contained in this document and that it is original and non plagiarized work of all the members of my group.

UT EID	Print Full Name	Signature	Date
<u>asp3642</u>	<u>Andreas Parrilha</u>		<u>4/28</u>
<u>Jes7564</u>	<u>Javier Sosa</u>		<u>4/28</u>
<u>jcw4938</u>	<u>Jack Walters</u>		<u>4/28</u>
<u>nay285</u>	<u>Nick Yanez</u>		<u>4/28</u>

ABSTRACT

This experiment investigated the impact of vortex generator (VG) placement on the aerodynamic performance of a NASCAR model, with the goal of reducing the coefficient of drag (C_D). Using a triangular VG geometry derived from an idealized design in existing literature, we tested configurations with VGs positioned at the front, middle, rear, and a visual-based location slightly behind the middle position, alongside a control case with no VGs. Tests were conducted in a wind tunnel at Reynolds numbers of $1.6 \times 10^5 \pm 1000$, $3.28 \times 10^5 \pm 1000$, $4.13 \times 10^5 \pm 1000$, $4.95 \times 10^5 \pm 1000$, and $6.58 \times 10^5 \pm 2000$. Flow behavior was analyzed through smoke trails and surface tufts to visualize boundary layer development and separation. Of all configurations, only the rear-mid placement produced a significant C_D reduction, decreasing drag by approximately 3% on average compared to the control. Front-mounted VGs, however, increased drag, due to elevated skin friction from early boundary layer energization. Other placements yielded negligible improvements or increased drag. These results highlight the importance of precise VG placement for effective drag reduction on bluff-body vehicles such as stock cars.

TABLE OF CONTENTS

ABSTRACT	page 2
INTRODUCTION	page 4
APPARATUS & PROCEDURE	page 7
RESULTS & DISCUSSION	page 9
SUMMARY & CONCLUSIONS	page 17
APPENDICES	page 19
REFERENCES	page 21

1. INTRODUCTION

Drag is an extremely important force to consider when analyzing race cars, as it can directly impact the performance of the vehicle. Large drag forces can dramatically decrease the net power output of an engine resulting in a slow car, regardless of how powerful its engine could be. Small aerodynamic modifications such as spoilers, diffusers, and vortex generators can drastically alter the aerodynamics of a car, resulting in a wide range of effects on the car's performance depending on how it was set up. These effects can mean the difference between winning and losing on the racetrack, and understanding how to mold the aerodynamics to work in our favor is something that applies to multiple fields beyond just racing cars.

Somewhat similar to blunt bodies, a big contributor to drag in racing cars is parasitic drag resulting from flow separation and the formation of a wake. This wake can be minimized by increasing the Reynolds number, or by inducing turbulence such as dimples on a golf-ball as seen with Fig. 1. Vortex generators are a well-known method for inducing turbulence in the boundary layer, but their effectiveness varies depending on placement and flow conditions. By inducing turbulence, the momentum of the boundary layer is replenished, follows the contour of a body's surface, and decreases the wake size [2]. They are often used on airfoils [1] to delay stall at high AoA and wind turbines [4] to maximize efficiency. In this lab we test multiple positions of vortex generators to find the optimal positioning for vortex generators on a NASCAR like stock racing car to minimize wake size and minimize power loss.

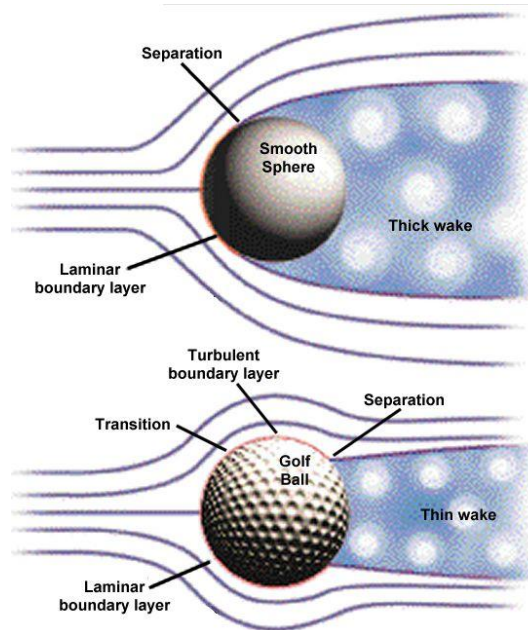


Figure 1: Effects of vortex generating dimples in a golf ball compared to a normal ball [5]

To make and analyze the airflow over a mock racing car, we make use of an open circuit wind tunnel provided by the Department of Aerospace Engineering and Engineering Mechanics. An open circuit wind tunnel lets us run our tests with known flow conditions, allowing us to fully analyze our car's flow characteristics and drag effects [6]. Open circuit wind tunnels are effective for small scale testing, as well as being much cheaper than their closed-circuit counterparts. The downsides for the open circuit design are that measurements by the wind tunnel are more prone to error since the system is susceptible to external influences such as fluctuations in ambient conditions, air disturbances, and inconsistencies in the airflow, as well as having a limit on the Reynolds number it can achieve.

By using the wind tunnel and dimensional scaling, we can accurately calculate and analyze the performance of a full scale car. This technique is the basis for a lot of research, allowing engineers to accurately aerodynamic behavior without the need for giant wind tunnels to test full scale models of aircraft, cars, and any other vehicles. For two models to be dimensionally scalable, they both must be geometrically similar and have matching Reynolds numbers. If these conditions match, then we can predict the behaviors of a larger model with a smaller one. The Reynolds number is defined as:

$$Re = \frac{\rho U_{\infty} L}{\mu} \quad (1)$$

where ρ is the fluid density, U_{∞} is the freestream velocity, L is the bumper-to-bumper length of the car, and μ is the dynamic viscosity of the fluid. Due to the low precision nature of our wind tunnel, we do have to calculate some of the properties of the air flow using some basic flow properties to get the smallest uncertainties possible for our Reynolds numbers calculations.

Derived from the ideal gas law, the equation for air density (ρ) is:

$$\rho = \frac{P_{atm}}{R_{Air} * T} \quad (2)$$

where P_{atm} is the atmospheric pressure, R_{Air} is the ideal gas constant for dry air, and T is the temperature of the airflow. Next, the viscosity (μ) is found with:

$$\mu = \frac{\mu_{ref} * T^{\frac{3}{2}}}{T + S} \quad (3)$$

where T is the temperature of the air in the wind tunnel, T_{ref} is a standardized reference temperature, μ_{ref} is the viscosity of air at the known reference temperature of T_{ref} , and S is Sutherland's temperature.

To make sure we had an effective experiment, we had to take both qualitative and quantitative measurements. The qualitative measurement was done with flow visualization, which allowed us to directly observe the effects that the vortex generators had on the fluid flow. Quantitative measurements were done with the pistol grip attachment, which let us directly measure the axial “drag” force that was affecting our model. These measurements, along with the Reynolds number, allowed us to directly find the coefficient of drag, coefficient of power loss, and make a clear conclusion about the effects of the vortex generator placement.

1.1 FLOW VISUALIZATION

As mentioned above, the vortex generators introduce turbulence to the airflow, drastically changing how it moves past the car. By using smoke trails and string tufts, we can actively observe how effective the vortex generators are at introducing the turbulence, infer where the ideal spot for the vortex generators are, as well as observing the boundary layer, flow separation, and wake formation. This is part of the qualitative data that lets us see exactly where the flow separation occurs, which is useful for comparing the effects with and without vortex generators.

1.2 COEFFICIENT OF DRAG

As the air flows over the car, a wake area will be created in certain regions of the car. This wake area creates a pressure gradient between the front and back of the car creating drag. The coefficient of drag is a normalized value of the drag force, meaning it can be used to compare drag between scales. The coefficient of drag is defined as:

$$C_D = \frac{F_D}{q_\infty * A_S} \quad (4)$$

where F_D is the drag force measured by the pistol grip, q is the dynamic pressure, and A_S is the cross-sectional area of our car model. With this value, we can compare the drag created by the small-scale model to a full-scale model.

1.3 COEFFICIENT OF POWER

The drag force would counteract the driving force of the engine as the car drove along a racetrack. This results in power loss from the engine, resulting in an overall slower car. Finding the effective change in power with the vortex generators at different spots would help us see how

effective they truly are. The power loss is defined as:

$$P = F_D * u_\infty \quad (5)$$

where F_D is the drag force measured by the pistol grip, u_∞ is the freestream velocity. This by itself is not useable as a comparison between scales, so we find the coefficient of power, which just like the coefficient of drag, can give us a value that is easily comparable to the full-scale model. The coefficient of power is found with:

$$C_P = \frac{P}{q_\infty * A_S * u_\infty} \quad (6)$$

where P is the power found above, u is the freestream velocity, q is the dynamic pressure, and A_S is the cross sectional area of the car.

2. APPARATUS & PROCEDURE

For our testing we used a roughly $\frac{1}{12}$ scaled down model of Lightning McQueen, a fictitious NASCAR like stock racing car. The car was $0.411 \pm 0.001\text{m}$ long, with a $0.021 \pm 0.001\text{m}^2$ cross sectional area. The car had tufts spread along its surface, with bald spots where the vortex generators would be placed. The car model had a space for the pistol grip to slot into and was permanently fixed on a flat position with its bottom plane parallel with the bottom surface of the wind tunnel. For our vortex generators, we used a strip of six pairs of vortex generators, each following the optimal design criteria [3], seen in Fig. 2.

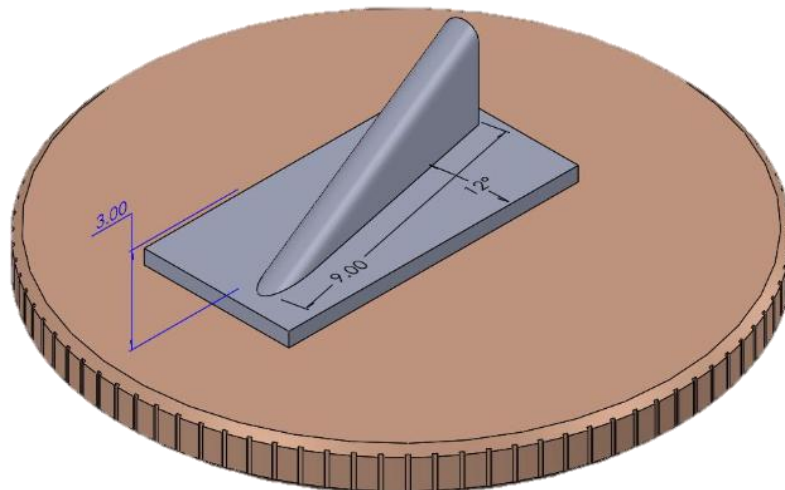


Figure 2: Vortex Generator dimensions with penny for reference [3]

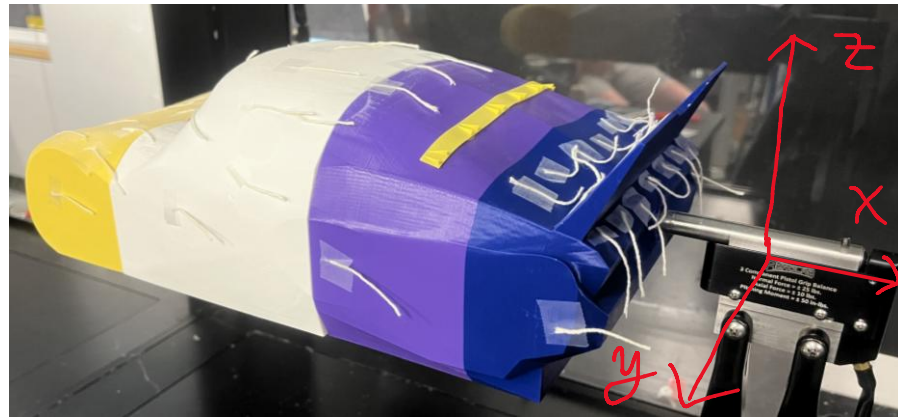


Figure 3: Experimental Setup with Vortex Generator in back position

There were five distinct set ups we had to test for this lab. We went from no vortex generators, vortex generators at the front, at the top by the windshield, in the back by the spoiler, and finally at the ideal position chosen at a promising spot halfway between the top and back positions. At each set up, we had the wind tunnel at Reynolds numbers of 1.6×10^5 , 3.28×10^5 , 4.13×10^5 , 4.95×10^5 , and $6.58 \times 10^5 \pm 1000$ (200, 400, 500, 600, and 800 RPM respectively), where we did flow visualization and measured the drag forces for a 5 second period at a sampling rate of 100 Hz. The resulting drag and power coefficients, as well as flow visualization images are presented in the following section.

3. RESULTS AND DISCUSSION

3.1 FLOW VISUALIZATION

Flow visualization was used to analyze the difference in flow patterns based on five different placements of the VG: front, middle, back, ideal, and a control group. For each configuration we tested five different fan speeds of 200, 400, 500, 600, and 800 RPM.

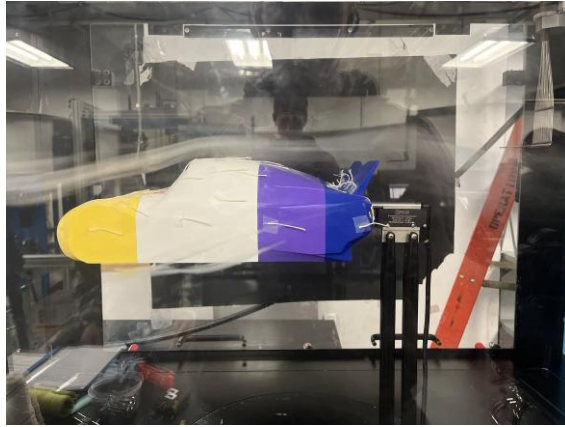


Figure 4: Control, 200 rpm

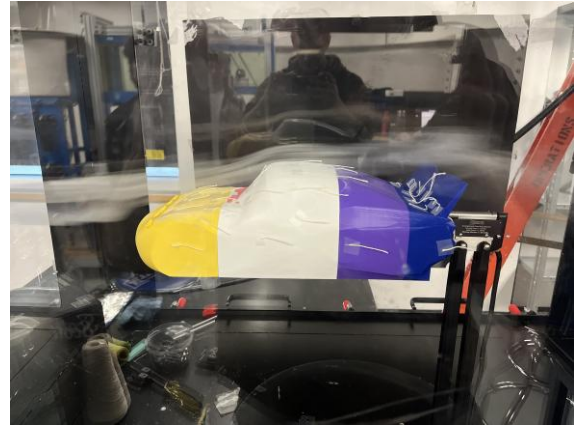


Figure 5: Front VG, 200 rpm

The flow in Fig. 4 is relatively calm with no vortices along the body, has a point of separation about 2/3 along the model, and has a slight wake in the back. As VGs are attached to the front in Fig. 5, vortices already begin to form towards the back and the flow is attached slightly longer than in the control group.

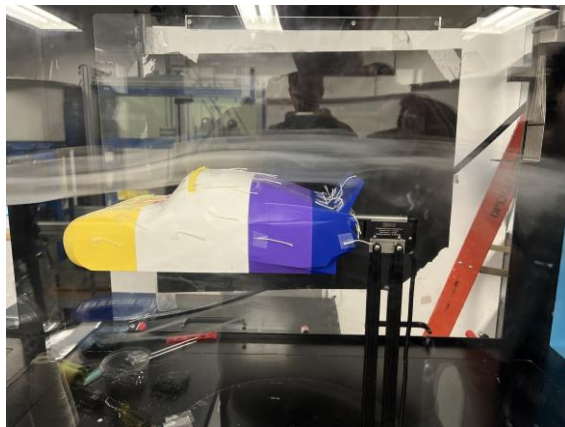


Figure 6: Middle VG, 200 rpm

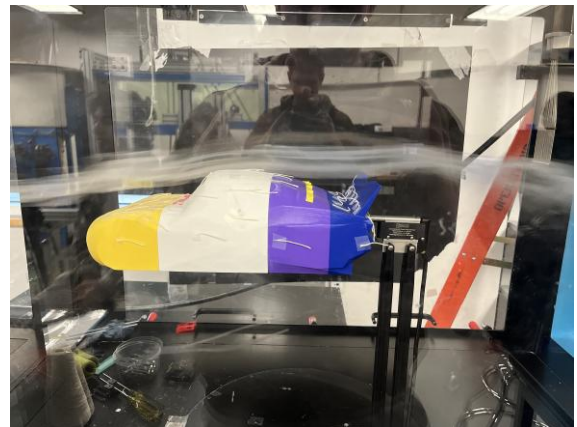


Figure 7: Back VG, 200 rpm

Fig. 6 shows VGs in the middle created a larger wake size and significantly more vortices as there is more circulation around the spoiler. With VGs attached to the back in Fig. 7, the vortices in the flow are created far past the spoiler.

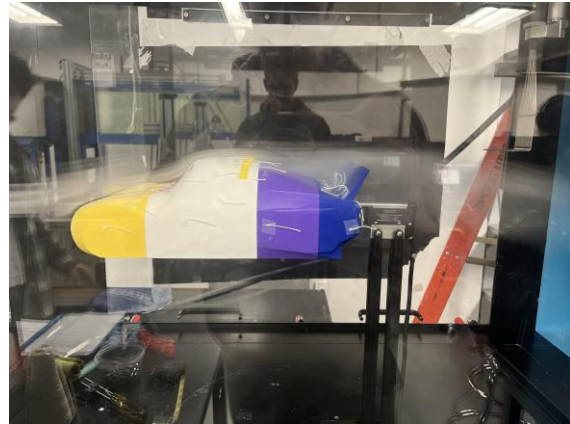


Figure 8: Ideal VG, 200 rpm

With the Ideal VG placement, Fig. 8 shows a controlled flow that is able to create vortices before the end of the model and keep the flow attached almost halfway through the purple section.

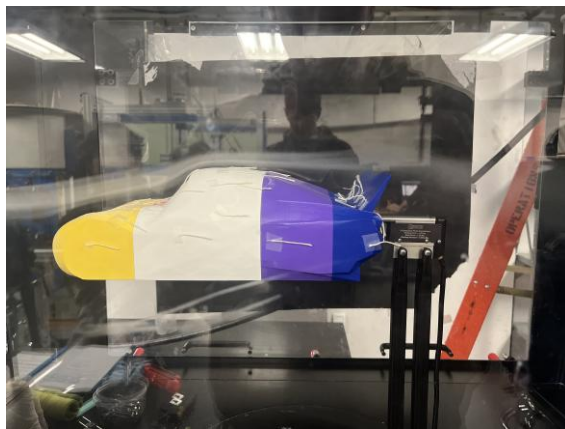


Figure 9: Control, 400 rpm

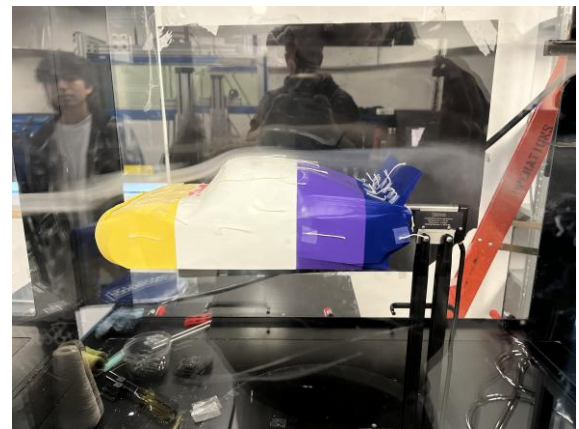


Figure 10: Front VG, 400 rpm

The flow in Fig. 9 is attached until about the beginning of the purple section, slight wake with little to no vortices. Fig. 10 has vortices forming directly after the spoiler and a point of separation about halfway through the purple section.

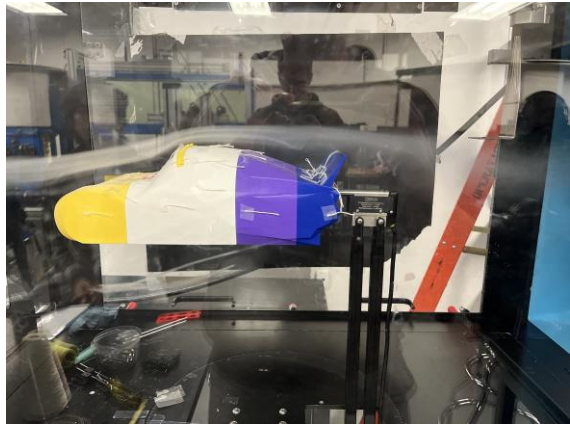


Figure 11: Middle VG, 400 rpm

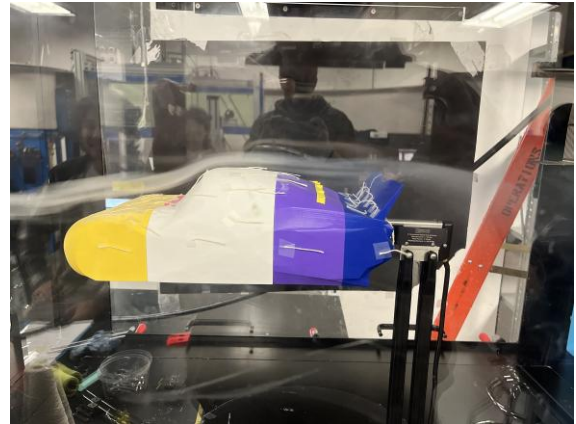


Figure 12: Back VG, 400 rpm

Fig. 11 has a separation point earlier than the control group at slightly before the purple section and a wake with vortices far behind the end of the model. The flow in Fig. 12 is attached until about right before where the VGs are placed and is more controlled along the body.

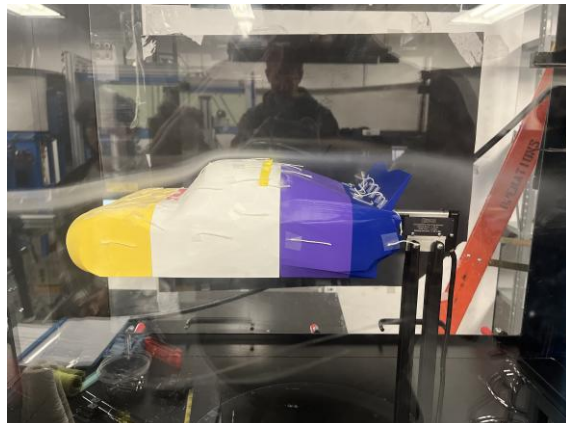


Figure 13: Ideal VG, 400 rpm

The flow in Fig. 13 proves to be ideal as it has the most controlled turbulence and smallest wake along the body.

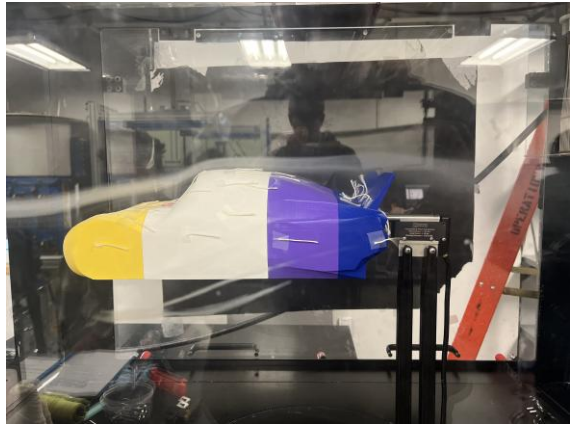


Figure 14: Control, 500 rpm

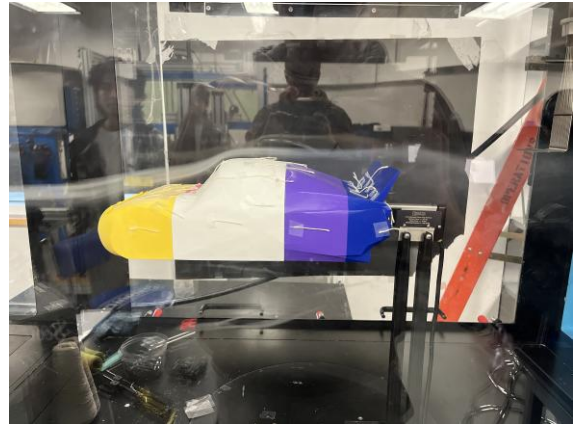


Figure 15: Front VG, 500 rpm

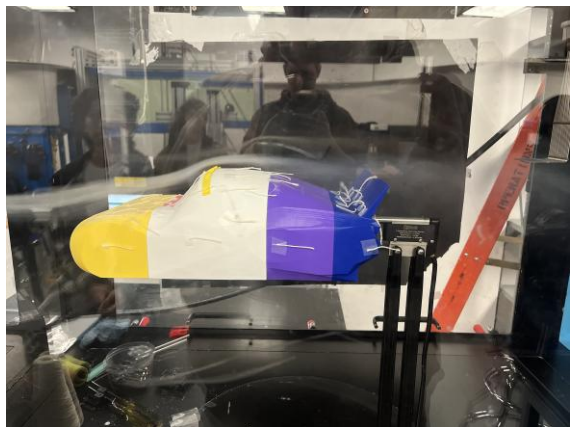


Figure 16: Middle VG, 500 rpm



Figure 17: Back VG, 500 rpm



Figure 18: Ideal VG, 500 rpm

As the speed increases to 500 RPM, the flow becomes harder to control and disturb. Figures 14 and 15 have the earliest point of separation at about the start of the purple section. Figures 16 and

18 have the latest point of separation at about halfway through the purple section. The ideal placement shows a controlled flow with the smallest wake size along the body.

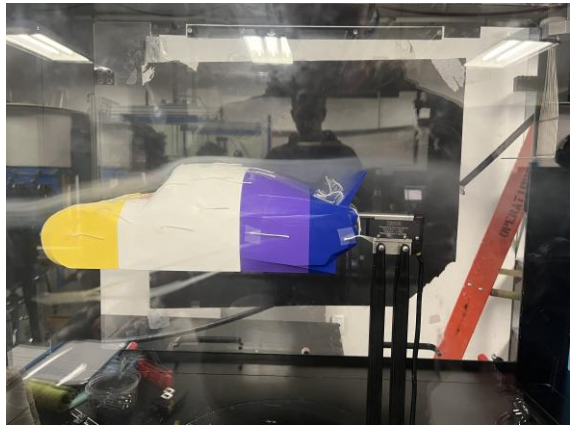


Figure 19: Control, 600 rpm

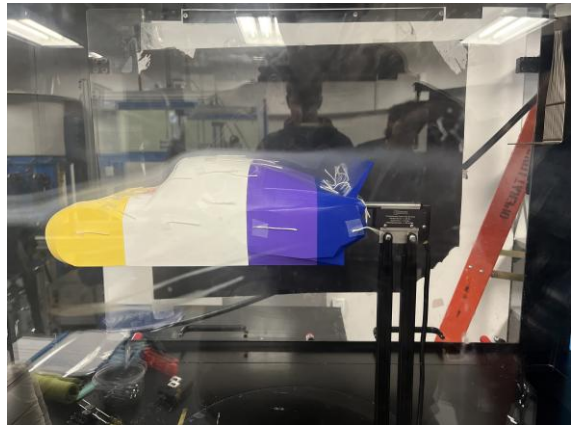


Figure 20: Front VG, 600 rpm

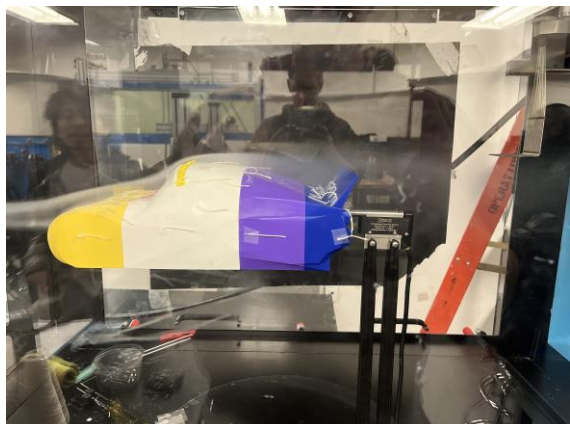


Figure 21: Middle VG, 600 rpm

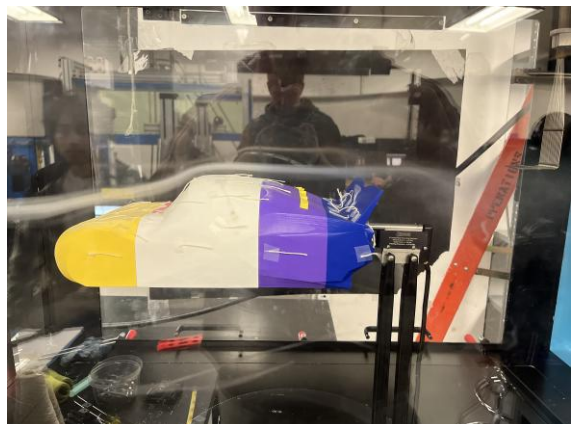


Figure 22: Back VG, 600 rpm

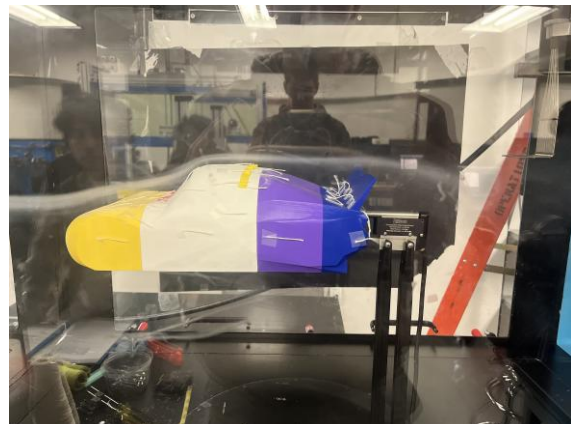


Figure 23: Ideal VG, 600 rpm

For all flows at 600 RPM, the separation point is very similar at about the start of the purple section. Figures 22 and 23 have controlled and smaller wakes.

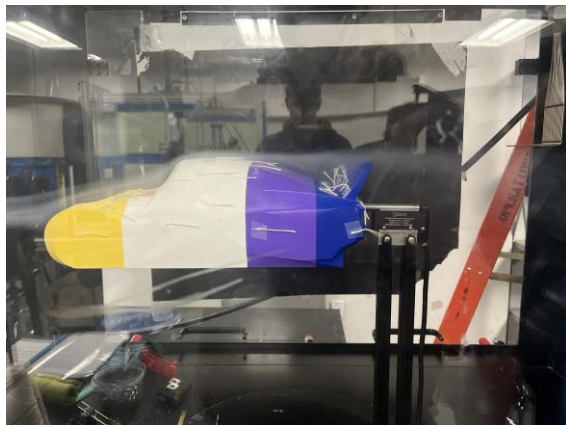


Figure 24: Control, 800 rpm

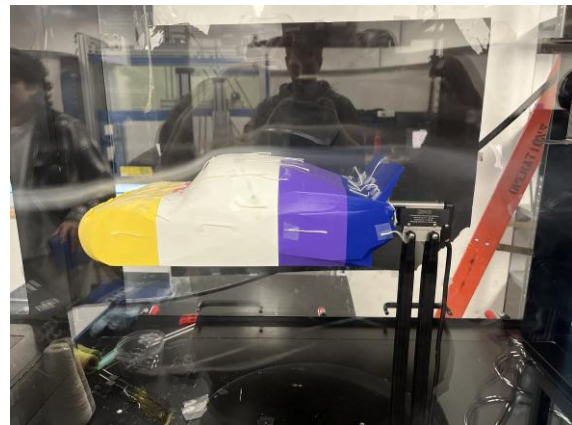


Figure 25: Front VG, 800 rpm



Figure 26: Middle VG, 800 rpm

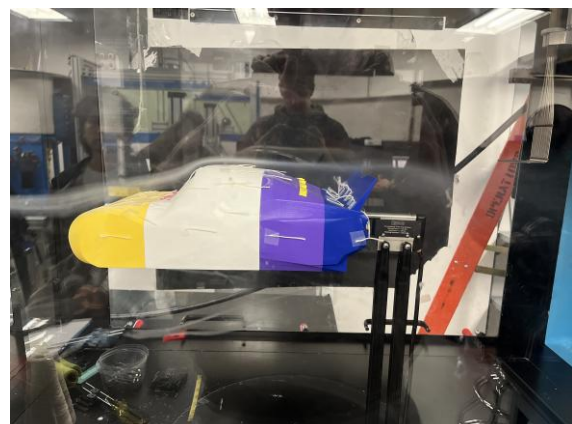


Figure 27: Back VG, 800 rpm



Figure 28: Ideal VG, 800 rpm

The control group in Fig. 24 has little to no wake past the spoiler while all other flows at 800 RPM show vortices forming slightly past the end of the model. Figures 27 and 28 show the most controlled flow with less circulation before the spoiler and smaller wakes.

3.2 WIND TUNNEL DRAG COEFFICIENT VS REYNOLD'S NUMBER

For this experiment, we looked at how the placement of vortex generators affected flow separation, which directly correlates to drag. To compare the results of this experiment, we plotted the coefficient of drag (C_d) against Reynold's number (Re) for five flow cases. These cases were a control which had no VG, an idealized placement based on our flow visualizations, and three more placements at the leading edge, mid-car, and trailing edge. By overlaying all C_d curves on the same graph, we can directly compare how each placement altered pressure-drag behavior as Reynold's number increases. From the graph we can see which placement leads to more drag, has no effect, or reduces drag. In short, this comparative view reveals which VG placement is most effective at each Re in reducing this drag.

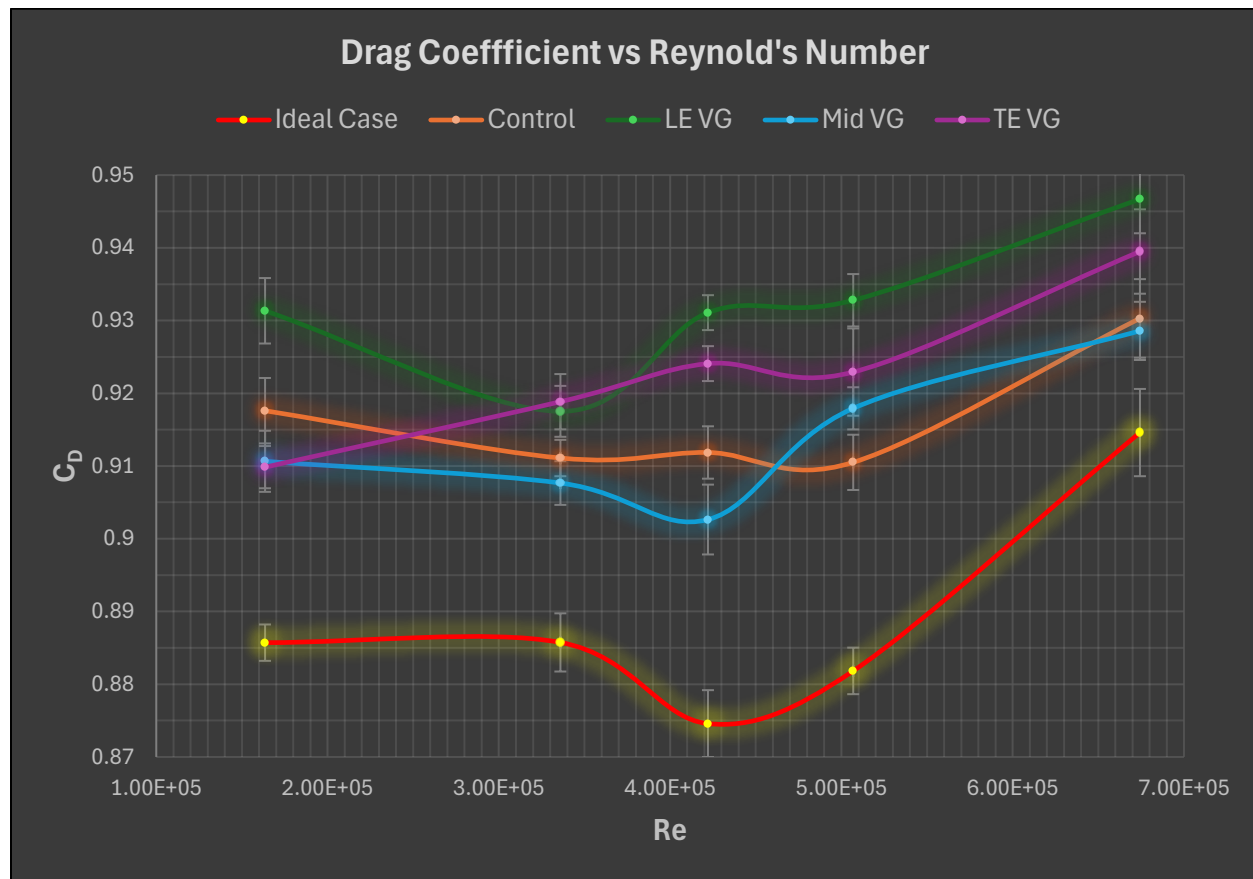


Figure 29: The 5 cases for vortex generator placements coefficients of drag plotted against Reynold's Number

From Fig. 29, we can see that our ideal placement reduced drag compared to our control. This would mean we succeeded in making sure our flow stayed attached for a longer period. The other cases either show almost no change in comparison to the control or even an increase in the drag. We see that although the change is to the hundredths place, even at these low Reynold's numbers, vortex generators do reduce drag when placed in the correct position.

3.3 WIND TUNNEL POWER LOSS COEFFICIENT VS REYNOLD'S NUMBER

We were not only interested in looking at drag and flow separation, but also taking it a step further and seeing how vortex generators affected power loss caused by these drag forces. In order to see these effects, we plotted the coefficient of power loss ($C_{p\text{loss}}$) against Reynold's number for both the ideal and control cases. We chose to only plot the ideal case because we only cared about how much power loss we reduced by adding our vortex generator. Comparing these two curves shows how much extra engine power is expended to overcome drag at various flow speeds.

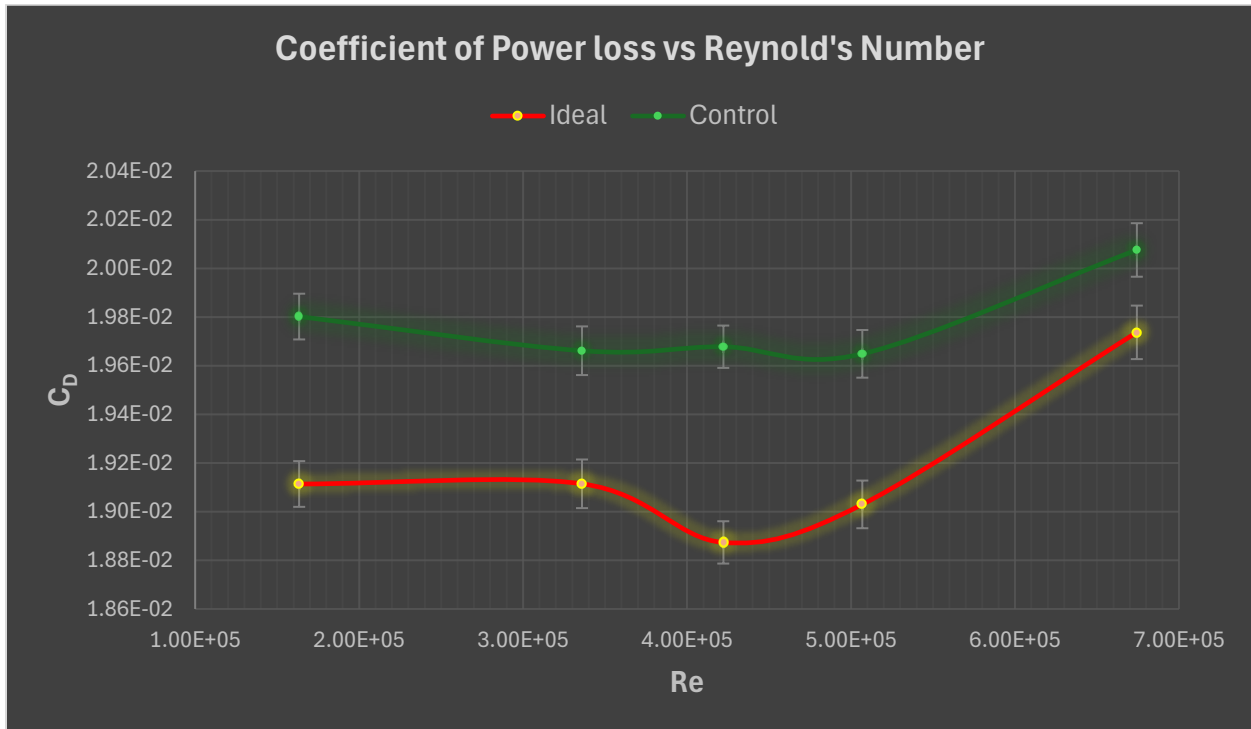


Figure 30: Ideal and control cases for vortex generator placements, coefficient of power loss plotted against Reynold's Number

We see from Fig. 30 that the same trend occurs compared to our drag vs Reynold's number plot. Which makes sense because the less drag, the less power wasted having to overcome that drag.

However, the power loss difference between the ideal case and the control is very minimal. This may mean the effect of the vortex generator at these Reynold's number is essentially negligible in practice.

4. SUMMARY & CONCLUSIONS

This study investigated the influence of vortex generator (VG) placement on the aerodynamic performance of a NASCAR model across a Reynolds number range of $1.6 \times 10^5 \pm 1000$ to $6.58 \times 10^5 \pm 2000$. Flow visualization using smoke trails and surface tufts showed that, at lower Reynolds numbers (200, 400, and 500 RPM), the control configuration exhibited flow separation shortly after the apex of the car (~65% body length), as shown in Figures 4-7. A region of high pressure formed between the hood apex and the spoiler, promoting early flow detachment. Placement of VGs at approximately 65% body length (the ideal location) delayed separation, maintaining flow attachment and allowing the air to penetrate the stagnant region (Fig. 8).

Drag coefficient (C_D) trends supported these visual observations. Between Reynolds numbers of approximately 1.6×10^5 and $4.13 \times 10^5 \pm 1000$, C_D decreased across most configurations, with the ideal VG placement consistently producing the lowest drag (Fig. 29). Beyond this regime, C_D began to increase again. In addition, the coefficient of power loss (C_P) followed a similar trend, although the absolute impact on power consumption was negligible—amounting to only a few watts for real-world power outputs.

One major limitation of this study was the inability to match the Reynolds numbers of a real NASCAR environment ($\sim 2.8 \times 10^7$), due to scale and speed constraints of the wind tunnel. As aerodynamic behavior can change significantly at higher Reynolds numbers, particularly regarding boundary layer transition, it cannot be assumed that the VG performance observed here would directly translate to full-scale vehicles. Future testing in high-speed facilities would be necessary to fully validate VG effectiveness at race conditions.

It is also important to note that due to the complex topologies of automotive bodies, separation points cannot be universally normalized based on vehicle length. Flow behavior is highly sensitive to surface features and geometry, limiting direct comparisons across different designs.

Overall, the results demonstrate that carefully placed vortex generators can meaningfully reduce drag by delaying flow separation under certain conditions. However, their effectiveness is strongly dependent on Reynolds number, local flow conditions, and vehicle-specific geometries.

APPENDICES

APPENDIX I: Lab Notes

Notes taken digitally:

Dimensions of Model

Length: 0.411 +/- 0.001 m

Largest Cross-Sectional Area: 0.021 +/- 0.001 m²

VG Placements

Front: 5%

Middle: 50%

Back: 80%

Ideal: 65%

APPENDIX II: Calibration Data

	200 RPM	400 RPM	500 RPM	600 RPM	800 RPM
Velocity [m/s]	5.98 +/- 0.02	12.28 +/- 0.04	15.44 +/- 0.02	18.52 +/- 0.03	24.61 +/- 0.05
Temperature [K]	296.27 +/- 0.09	295.88 +/- 0.09	295.34 +/- 0.09	295.92 +/- 0.09	296.16 +/- 0.09
Dynamic Pressure [Pa]	21.31 +/- 0.12	89.49 +/- 0.64	141.60 +/- 0.43	203.63 +/- 0.66	359.77 +/- 1.46
Reynold's Number	1.60×10^5 +/- 1000	3.28×10^5 +/- 1000	4.13×10^5 +/- 1000	4.95×10^5 +/- 1000	6.58×10^5 +/- 2000

REFERENCES

- [1] Gutiérrez, R., et al. (2020). *Wind tunnel tests for vortex generators mitigating leading-edge roughness on a 30% thick airfoil*. Journal of Physics: Conference Series, 1618, 052058. <https://doi.org/10.1088/1742-6596/1618/5/052058>
- [2] J. Anderson, *Fundamentals of aerodynamics.*, 6th ed. McGraw-Hill, 2016. Available: <https://aviationdose.com/wp-content/uploads/2020/01/Fundamentals-of-aerodynamics-6-Edition.pdf>
- [3] Omar Madani Fouatih, Marc Medale, Omar Imine, Bachir Imine, *Design optimization of the aerodynamic passive flow control on NACA 4415 airfoil using vortex generators*, European Journal of Mechanics - B/Fluids, Volume 56, 2016, Pages 82-96, ISSN 0997-7546, <https://doi.org/10.1016/j.euromechflu.2015.11.006>
- [4] Zhenzhou Zhao, Ruifang Jiang, Junxin Feng, Huiwen Liu, Tongguang Wang, Wenzhong Shen, Ming Chen, Dingding Wang, Yige Liu, *Researches on vortex generators applied to wind turbines: A review*, Ocean Engineering, Volume 253, 2022, 111266, ISSN 0029-8018, <https://doi.org/10.1016/j.oceaneng.2022.111266>
- [5] J. Scott, “Aerospaceweb.org | Ask Us - Golf Ball Dimples & Drag,” aerospaceweb.org, Feb. 13, 2005. <https://aerospaceweb.org/question/aerodynamics/q0215.shtml>
- [6] Tinney, C.E. (2020) ASE120k Laboratory Handbook. Dept of Aerospace Engineering and Engineering Mechanics at The University of Texas at Austin.
- [7] “Lightning McQueen,” Piston Cup Wiki. https://piston-cup.fandom.com/wiki/Lightning_McQueen